Supplemental Material: "Parameterization of an effective potential for protein-ligand binding from host-guest affinity data"

Lauren Wickstrom[1]*, Nanjie Deng[2], Peng He[2], Ahmet Mentes[2], Crystal Nguyen[3], Michael K. Gilson[3], Tom Kurtzman[4], Emilio Gallicchio[5], and Ronald M. Levy[2]

[1] Borough of Manhattan Community College, The City University of New York, Department of Science, New York, NY 10007; [2]Center for Biophysics & Computational Biology/ICMS, Department of Chemistry, Temple University, Philadelphia, PA 19122; [3]Skaggs School of Pharmacy and Pharmaceutical Sciences, University of California San Diego, La Jolla, CA 92093-0736, USA; [4]Department of Chemistry, Lehman College, The City University of New York, Bronx, NY 10468; [5]Department of Chemistry, Brooklyn College, the City University of New York, Brooklyn, NY 11210.

I Methods and Materials

A. Parameterization details

1) β-CD cavity

The locations of the hydration sites for β-CD, which are the same in the prior study (Wickstrom et al. 2013), were selected based on the symmetry and topology of the cavity. Non-polar hydration sites were placed as offsets of the C-H bond vectors pointing into the β-CD cavity. Each glucose monomer was assigned two hydration sites, since there are two non-polar C-H bonds in each glucose monomer. Since there are 7 monomers in β-CD, the cavity contained a total of 14 hydration sites (Figure 4 and S4). This placement maintained the 7-fold symmetry of the β-CD molecule, while occupying the region most relevant to binding.

2) Carboxylate group

The locations of the hydration sites on the carboxylate functional group were selected based on the local topology of hydrogen bond acceptor atoms of the solute in the original AGBNP2 paper (Gallicchio, Paris, and Levy 2009). The carboxylate group geometry exhibits a trigonal planar geometry where each oxygen is a hydrogen bond acceptor. While the initial results for these hydration sites were promising (Gallicchio, Paris, and Levy 2009) , two additional hydration sites were later added to each carboxylate oxygen to account for potential hydrogen bonds formed in an out of the plane with water (unpublished results). Thus, there are four hydration spheres positioned around each carboxylate oxygen (Figure S1), for a total of 8 hydration sites per carboxylate group.

The solute-solvent hydrogen bond correction energy parameter, h_w, was initially set to -1.25 kcal/mol for each of the 8 hydration sites located around the carboxylate group. Using this initial h_w parameter, we calculated the contributions of the solvation free energy to the binding affinity. Based on analysis of the structural ensembles of β-CD+carboxylate guests, we

estimated that, for each guest carboxylate, 4 out of the 8 water sites are occupied by the atoms of the host in the bound state, and therefore do not contribute to the solute-solvent interactions. Thus, this hydrogen bond contribution disfavors the bound state over the unbound state by approximately 5.0 kcal/mol, which is a significant effect. Because the initial calculations led to underestimates of the binding affinities of carboxylate-containing guests in particular, we reduced h_w for the carboxylate oxygen sites from -1.25 to to -0.75 kcal/mol, thus reducing the desolvation penalty to 3 kcal/mol on average and enhancing the calculated binding affinities by about 2 kcal/mol, relative to calculations with the original carboxylate parameters, as detailed below.

B. Analysis

1) GIST of β-CD and hexanoate molecules

We investigated the hydration properties of the separate β-CD and hexanoate molecules using Grid Inhomogeneous Solvation Theory (GIST) analysis (Nguyen, Young, and Gilson 2012). For each molecule, a molecular dynamics simulation was performed in a TIP3P(Jorgensen et al. 1983) cubic water box, using the DESMOND package (Bowers et al. 2006). Position restraints were used on all of the heavy atoms of the β-CD with a force constant of 8.0 kcal/mol/Å^2 , which allowed for free rotation of hydrogens. Position restraints were used on all atoms of hexanoate with a force constant of 8.0 kcal/mol/Å^2. The MD simulations were run for 100 ns and snapshots were collected every .5 ps. GIST was implemented on a cubic grid with spacing of 0.5 Å along each axis and dimensions 20.5 Å X 20.5 Å X 20.5 Å. GIST maps were visualized using the program visual molecular dynamics (VMD) (Humphrey, Dalke, and Schulten 1996).

2) Binding free energy analysis

BEDAM is based on the binding energy function u, which corresponds to turning on the interactions between the host and the guest in a fixed conformation of the complex. The standard binding free energies were calculated using multistate Bennett acceptance ratio (MBAR) with binding energy distributions obtained from the simulations (Shirts and Chodera 2008). For the MBAR analysis, we employed the code provided by John Chodera and Michael Shirts (http://alchemistry.org). For the β-CD host-guest systems, statistical uncertainties were obtained using block bootstrap analysis (Chernick, 2008) with 100 blocks and 50 resampling trials for the last 3 ns of each BEDAM simulation. The standard deviation, referred to as error in the Supplemental Information, is reported based on the averages from 50 resampling trials. For the two HIV-PR complexes, the error bars are estimated by block averaging by dividing the full trajectory into 5 blocks. We also monitored the time evolution of the binding free energy for each BEDAM simulation to ensure the convergence of each free energy simulation (Figures S2 and S3).

3) Thermodynamic decomposition

The binding free energy can be expressed as the sum of the reorganization free energy and the average binding energy (Gallicchio and Levy 2011),

$$\Delta G^{\circ}_{\text{bind}} = \Delta E_{\text{bind}} + \Delta G^{\circ}_{\text{reorg}} \qquad (3)$$

The average binding energy, ΔE_{bind}, is equal to the average, $\langle u \rangle_1$, of the binding energy function in the ensemble of conformations of the complex in the coupled state ($\lambda = 1$). The binding energy, ΔE_{bind}, accounts for the change in the effective potential energy, which includes direct non-covalent interactions (electrostatic and van der Waals) as well as the net desolvation of the binding partners. The reorganization free energy ($\Delta G^{\circ}_{\text{reorg}}$) accounts for energetic strain

and change in the conformational entropy upon binding for the ligand and receptor. ΔG°_{reorg} is computed as the difference between the computed binding free energy and the average binding energy:

$$\Delta G^{\circ}_{reorg} = \Delta G^{\circ}_{bind} - \langle u \rangle_1 \qquad (4)$$

where $\langle u \rangle_1$ is the average binding energy in λ=1 state and ΔG°_{bind} is the standard binding free energy.

4) Conformational analysis of β-CD

The bound ensemble of the β-CD host-guest systems was characterized using two structural observables: (1) the orientation of the guest in the beta-CD cavity and (2) hydrogen bonding between the host and the guest (Table S4). The orientation is defined as the position of the carboxylate group on the guest relative to the different alcohol groups on the host. When the polar carboxylate is closer to the wider rim of β-CD laced with secondary alcohols, it is referred to as an up-state binder. If the carboxylate group is closer to the smaller rim of β-CD, it is characterized as a down-state binder. Further description of this structural characterization is included in our previous work (Wickstrom et al. 2013). These binding modes were further characterized based on possible hydrogen bond interactions between the polar group and the hydroxyl oxygen. Hydrogen bonds were defined using a distance cutoff of 4.0 Å between the carbon atom of the carboxylate group and the oxygen of the hydroxyl group.

FIGURE S1 Hydration sites around one oxygen of a carboxylate group, with two hydration sites in the carboxylate plane, and two out of the plane. The other oxygen was assigned analogous hydration sites, but they are not shown here, for the sake of clarity.

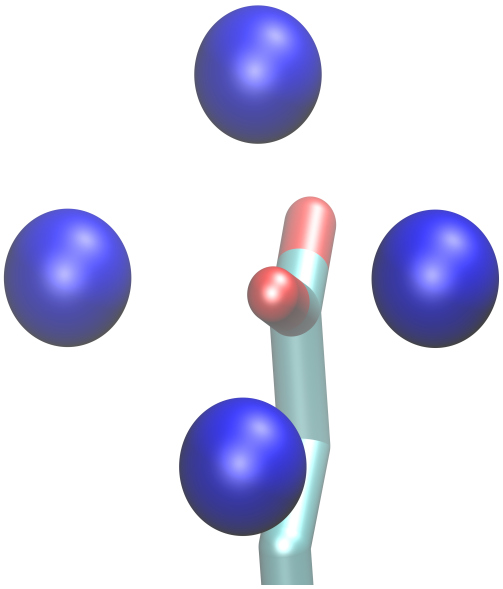

FIGURE S2 Binding free energy vs simulation time for heptanoate (black), phenylacetate (red), R-2-phenylbutyric acid (green), 1-napthaleneacetate (blue), N-t-boc-alanine (yellow) and 1R-3S-camphoric acid (brown) using the new carboxylate parameters for the AGBNP2 implicit solvent model.

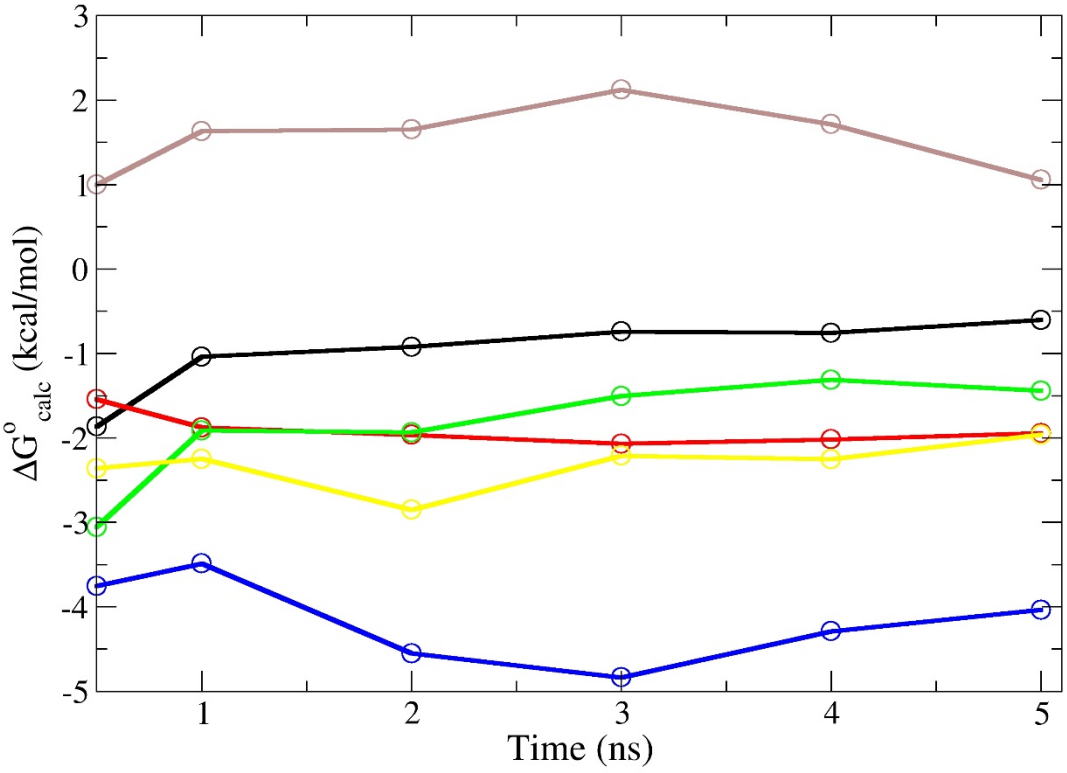

FIGURE S3 Binding free energy vs simulation time for the HIV allosteric inhibitors 1FN (black) and 1F1-N (red).

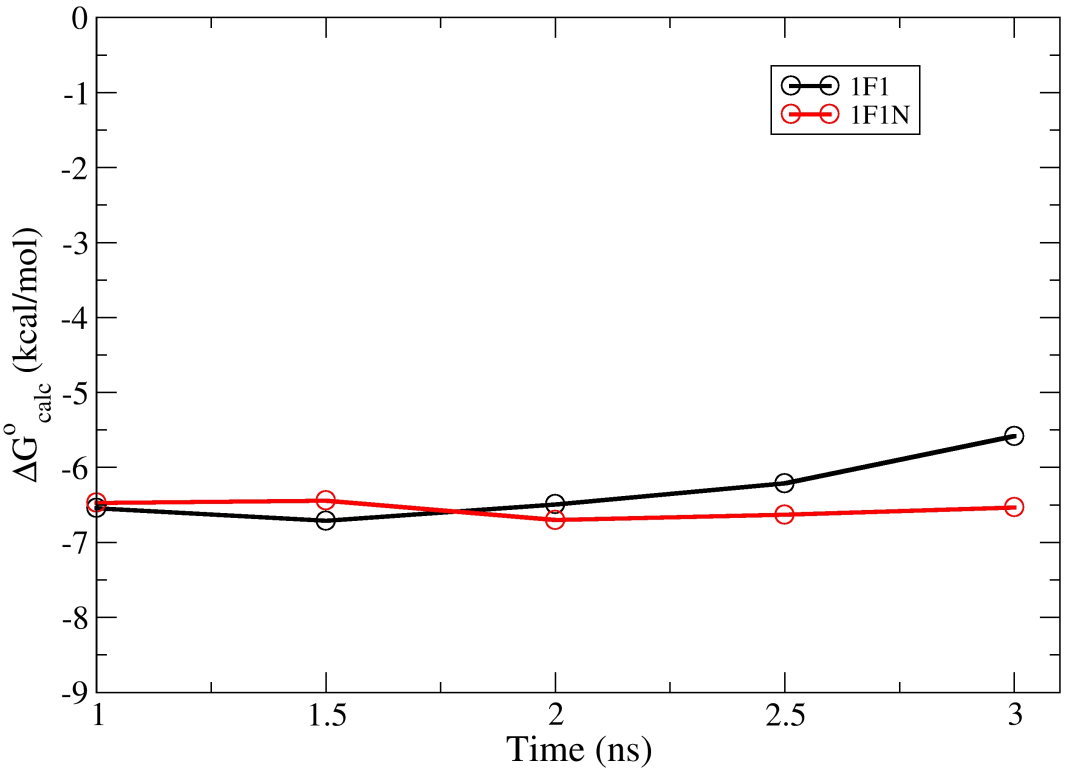

FIGURE S4 Hydration sites (blue) located in the cavity of β-CD.

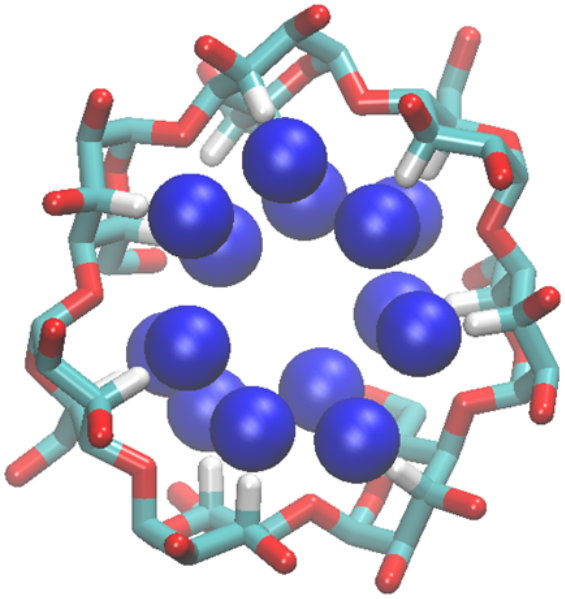

TABLE S1 2D chemical structures of the 33 guests with carboxylate functional groups.

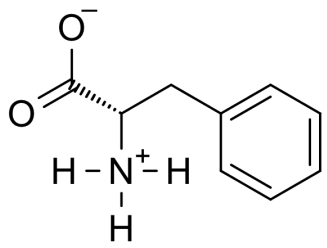	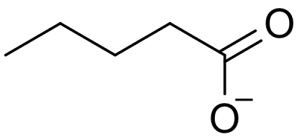
L-phenylalanine	pentanoate
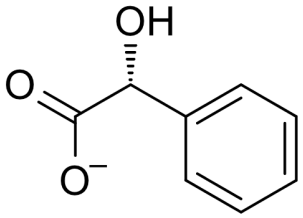	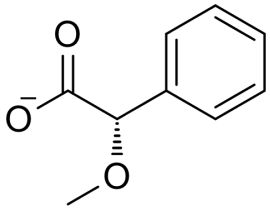
(R)-α-methoxyphenylacetic acid	(R)-mandelic acid
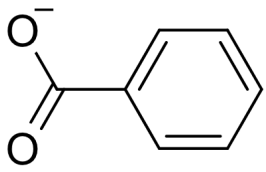	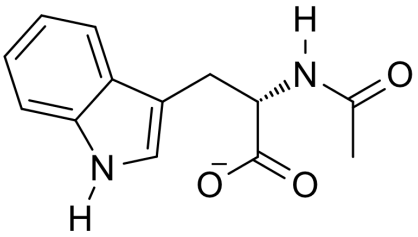
benzoate	N-acetyl-L-tryptophan
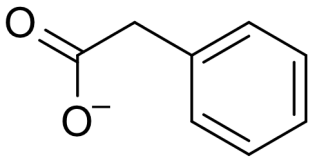	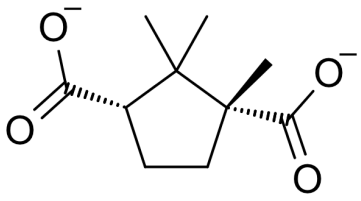
phenylacetate	1R-3S-camphoric acid

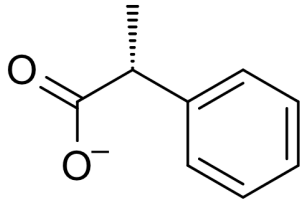	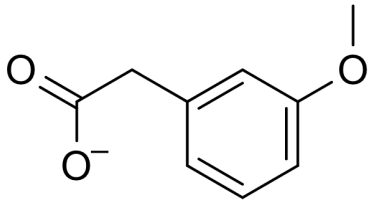
(R)-2-phenylpropionic acid	3-methoxyphenylacetate
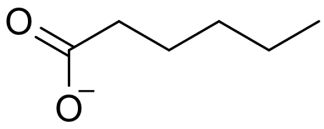	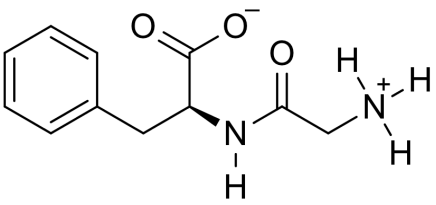
hexanoate	Gly-L-Phe
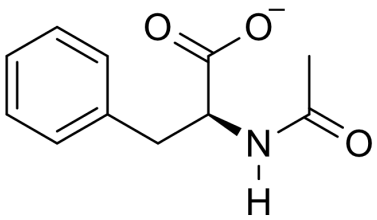	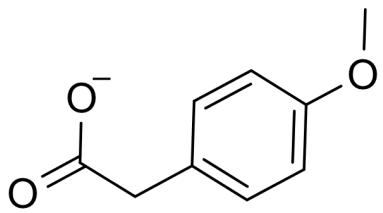
N-acetyl-L-phenylalanine	4-methoxyphenylacetate
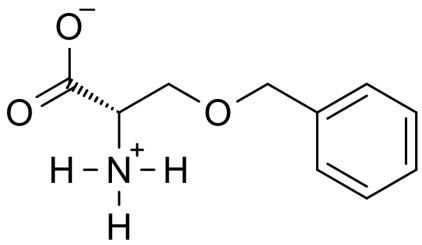	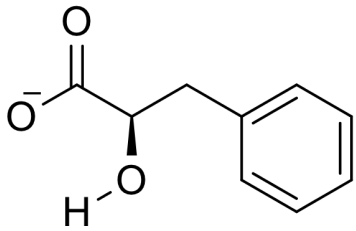
O-benzyl-L-serine	(R)-phenyllactic acid

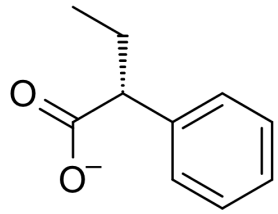	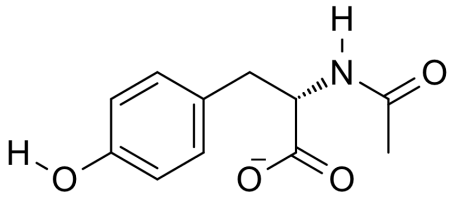
(R)-2-phenylbutyric acid	N-acetyl-L-tyrosine
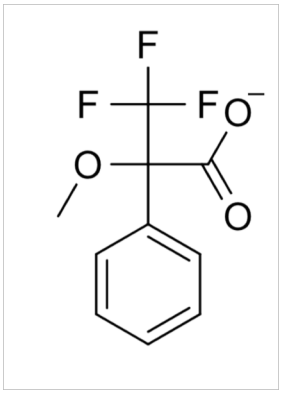	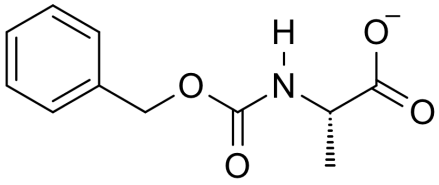
(S)-α-methoxy-α-trifluoromethylphenylacetic acid	N-Cbz-L-alanine
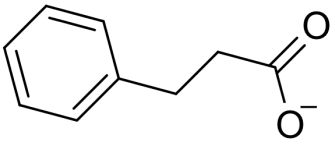	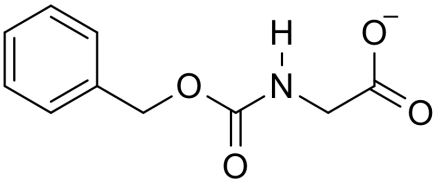
3-phenylpropionate	N-Cbz-glycine
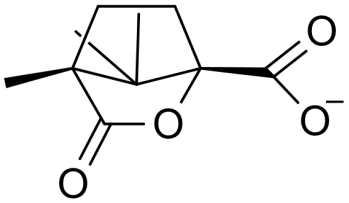	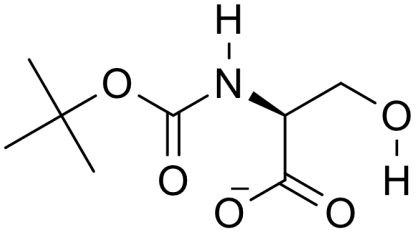
(R)-camphanic acid	N-t-Boc-L-serine

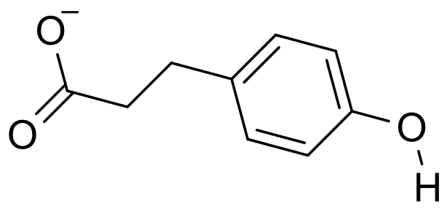	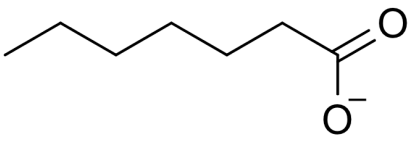
3-(4-hydroxyphenyl)propionate	heptanoate
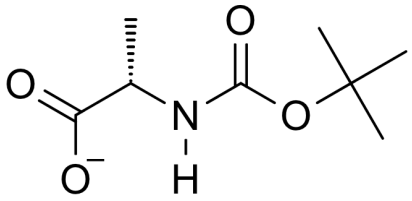	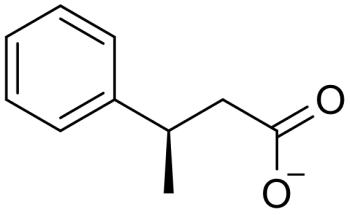
N-t-Boc-L-alanine	(R)-3-phenylbutyric acid
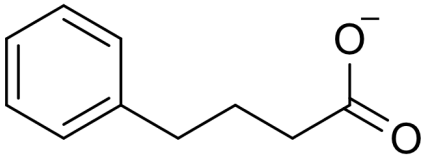	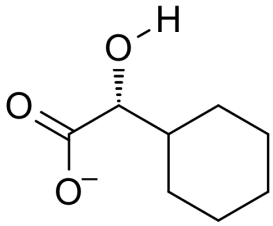
4-phenylbutanoate	(R)-hexahydromandelic acid
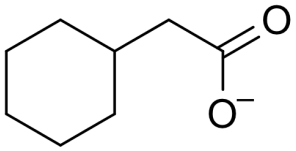	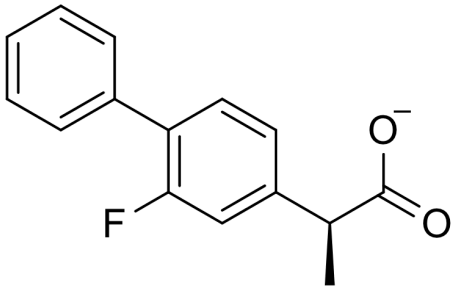
cyclohexylacetic acid	flurbiprofen

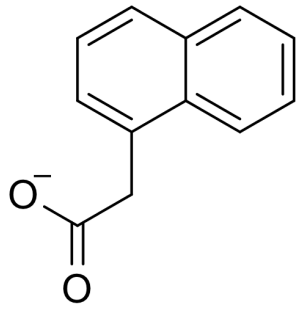	
1-naphthaleneacetate	

TABLE S2 Calculated and experimental binding free energy data(M. V. Rekharsky and Inoue 1998; M. Rekharsky and Inoue 2000; M. V. Rekharsky and Inoue 2002) for the host-guest systems using the original and optimized AGBNP2 parameter sets. The statistical error is calculated using a block bootstrap procedure described in the methods. The initial test set compounds listed in bold font.

Guests	ΔG_{exp}	$\Delta G_{calc\text{-}original}$**(error)**	$\Delta G_{calc\text{-}optimized}$**(error)**
L-phenylalanine	-0.72	3.62(0.06)	2.90(0.07)
pentanoate	-1.27	2.14(0.09)	0.24(0.05)
(R)-α-methoxyphenylacetic acid	-1.41	-0.05(0.10)	-1.56(0.10)
(R)-mandelic acid	-1.41	-0.53(0.09)	-1.53(0.06)
benzoate	-1.64	1.64(0.06)	0.34(0.05)
N-acetyl-L-tryptophan	-1.68	-1.53(0.16)	-3.05(0.11)
phenylacetate	-1.70	-0.41(0.11)	-2.01(0.07)
1R-3S-camphoric acid	-1.75	4.33(0.14)	1.64(0.14)
(R)-2-phenylpropionic acid	-2.09	-0.28(0.16)	-1.78(0.08)
3-methoxyphenylacetate	-2.16	-0.30(0.26)	-1.51(0.10)
hexanoate	-2.28	0.96(0.14)	-0.42(0.08)
Gly-L-Phe	-2.37	1.83(0.14)	-0.30(0.10)
N-acetyl-L-phenylalanine	-2.50	0.43(0.08)	-1.14(0.10)
4-methoxyphenylacetate	-2.51	-0.55(0.15)	-1.61(0.10)
O-benzyl-L-serine	-2.51	1.02(0.08)	0.94(0.06)
(R)-phenyllactic acid	-2.65	-0.05(0.13)	-1.59(0.06)
(R)-2-phenylbutyric acid	-2.69	0.00(0.17)	-1.42(0.08)
N-acetyl-L-tyrosine	-2.89	1.19(0.12)	-0.74(0.13)
(S)-α-methoxy-α-trifluoromethylphenylacetic acid	-2.93	-1.87(0.17)	-3.34(0.08)
N-Cbz-L-alanine	-2.96	-0.63(0.15)	-1.78(0.13)
3-phenylpropionate	-2.98	-0.38(0.13)	-1.17(0.08)
N-Cbz-glycine	-3.00	-0.26(0.07)	-1.07(0.08)
(R)-camphanic acid	-3.07	1.01(0.24)	-0.12(0.10)
N-t-Boc-L-serine	-3.35	0.50(0.09)	-1.26(0.14)
3-(4-hydroxyphenyl)propionate	-3.37	1.04(0.11)	-0.66(0.11)
heptanoate	-3.40	0.63(0.13)	-0.70(0.11)
N-t-Boc-L-alanine	-3.50	-0.41(0.18)	-2.14(0.11)

(R)-3-phenylbutyric acid	-3.55	0.67(0.10)	-1.37(0.08)
4-phenylbutanoate	-3.60	-0.74(0.13)	-1.87(0.08)
(R)-hexahydromandelic acid	-3.84	-0.12(0.11)	-2.54(0.11)
cyclohexylacetic acid	-4.23	-0.48(0.13)	-2.06(0.05)
flurbiprofen	-4.97	-3.19(0.13)	-4.38(0.10)
1-naphthaleneacetate	-5.93	-3.00(0.22)	-4.39(0.14)

Calculated values shown are $\Delta G_{exp,}$ the experimental binding affinity; $\Delta G_{calc\text{-}original,}$ the calculated binding affinity using the original carboxylate parameters; and $\Delta G_{calc\text{-}optimized,}$ the calculated binding affinity using the optimized carboxylate parameters All values are expressed in kcal/mol.

TABLE S3 Thermodynamic decomposition of the binding free energies for the host-guest systems using the original and optimized AGBNP2 parameter sets. The statistical error is calculated using a block bootstrap procedure described in the methods.

Guests	**$\Delta E_{bind-original}$ (error)**	**$\Delta E_{bind-optimized}$ (error)**	**$\Delta G°_{reorg-original}$ (error)**	**$\Delta G°_{reorg-optimized}$ (error)**
L-phenylalanine	-4.55(0.16)	-11.51(0.72)	8.17(0.22)	14.42(0.79)
pentanoate	-13.62(0.65)	-21.13(0.47)	15.76(0.74)	21.37(0.52)
(R)-α-methoxyphenylacetic acid	-20.67(0.15)	-23.30(0.28)	20.61(0.25)	21.73(0.38)
(R)-mandelic acid	-20.93(0.26)	-22.07(0.16)	20.40(0.35)	20.54(0.22)
benzoate	-9.74(0.25)	-14.66(0.27)	11.39(0.31)	14.99(0.32)
N-acetyl-L-tryptophan	-20.94(0.59)	-27.63(0.46)	19.40(0.75)	24.59(0.57)
phenylacetate	-19.32(0.13)	-24.24(0.75)	18.91(0.24)	22.23(0.82)
1R-3S-camphoric acid	-29.66(0.46)	-32.84(0.68)	34.00(0.60)	34.48(0.82)
(R)-2-phenylpropionic acid	-19.97(0.29)	-24.59(0.54)	19.69(0.45)	22.81(0.62)
3-methoxyphenylacetate	-21.19(0.50)	-23.20(0.27)	20.88(0.76)	21.69(0.37)
hexanoate	-16.71(0.57)	-21.77(0.57)	17.66(0.71)	21.34(0.65)
Gly-L-Phe	-19.43(1.02)	-22.45(0.24)	21.26(1.16)	22.14(0.34)
N-acetyl-L-phenylalanine	-14.47(0.61)	-22.42(0.23)	14.90(0.69)	21.28(0.33)
4-methoxyphenylacetate	-19.78(0.29)	-21.88(0.25)	19.23(0.44)	20.27(0.35)
O-benzyl-L-serine	-7.84(0.07)	-8.24(0.15)	8.86(0.15)	9.18(0.21)
(R)-phenyllactic acid	-16.74(0.88)	-25.71(0.62)	16.68(1.01)	23.87(0.68)
(R)-2-phenylbutyric acid	-19.15(0.20)	-23.27(0.43)	19.15(0.37)	21.86(0.51)
N-acetyl-L-tyrosine	-17.80(0.52)	-26.04(0.49)	18.98(0.64)	25.29(0.62)
(S)-α-methoxy-α-trifluoromethylphenylacetic acid	-23.48(0.14)	-33.55(1.08)	21.61(0.31)	30.22(1.16)
N-Cbz-L-alanine	-16.13(0.95)	-22.98(0.80)	15.50(1.10)	21.19(0.93)
3-phenylpropionate	-16.03(0.76)	-23.93(0.85)	15.65(0.89)	22.76(0.93)
N-Cbz-glycine	-10.25(0.32)	-16.33(0.91)	9.99(0.39)	15.27(0.99)
(R)-camphanic acid	-18.19(0.86)	-22.00(0.19)	19.20(1.10)	21.88(0.29)
N-t-Boc-L-serine	-16.93(0.67)	-26.63(0.36)	17.43(0.76)	25.37(0.50)
3-(4-hydroxyphenyl)propionate	-15.16(0.85)	-26.14(0.66)	16.20(0.96)	25.49(0.77)
heptanoate	-12.65(0.82)	-20.67(0.63)	13.28(0.95)	19.98(0.74)
N-t-Boc-L-alanine	-20.62(0.54)	-27.27(0.38)	20.21(0.72)	25.13(0.49)
(R)-3-phenylbutyric acid	-12.50(0.60)	-25.73(0.59)	13.18(0.70)	24.36(0.67)
4-phenylbutanoate	-15.27(0.90)	-23.48(0.63)	14.53(1.03)	21.61(0.71)
(R)-hexahydromandelic acid	-17.71(0.52)	-28.92(0.83)	17.59(0.63)	26.38(0.94)
cyclohexylacetic acid	-18.40(0.29)	-22.37(0.50)	17.92(0.42)	20.31(0.55)
flurbiprofen	-21.38(0.94)	-26.59(0.21)	18.19(1.07)	22.21(0.31)
1-naphthaleneacetate	-26.02(0.14)	-27.95(0.26)	23.03(0.36)	23.56(0.40)

Calculated values shown are $\Delta E_{\text{bind-original}}$, the binding energies for the original parameter set; $\Delta E_{\text{bind-optimized}}$, the binding energies for the optimized parameter set; $\Delta G_{\textbf{reorg,-original}}$,the reorganization free energy for the original parameter set; and $\Delta G_{\textbf{reorg,-optimized}}$,the reorganization free energy for the optimized parameter set. All values are expressed in kcal/mol.

TABLE S4 Populations of different binding modes of β-CD host-guest systems. Data in the parentheses used the original parameter set.

Guests	DS	H-bond DS	US	H-bond US
L-phenylalanine	0.00(0.01)	0.00(0.00)	1.00(0.99)	0.70(0.11)
pentanoate	0.53(0.00)	0.53(0.00)	0.47(1.00)	0.46(0.86)
benzoate	0.05(0.00)	0.05(0.00)	0.95(1.00)	0.92(0.80)
R-methoxyphenylacetic-acid	0.00(0.00)	0.00(0.00)	1.00(1.00)	1.00(0.99)
R-mandelic-acid	0.00(0.00)	0.00(0.00)	1.00(1.00)	0.99(0.97)
N-acetyl-L-tryptophan	0.00(0.00)	0.00(0.00)	1.00(1.00)	0.98(0.73)
phenylacetate	0.40(0.02)	0.40(0.02)	0.60(0.98)	0.60(0.96)
1R-3S-camphoric-acid	0.09(0.00)	0.09(0.00)	0.91(1.00)	0.80(0.63)
R-2-phenylpropionic-acid	0.40(0.00)	0.40(0.00)	0.60(1.00)	0.60(0.99)
3-methoxyphenylacetate	0.00(0.02)	0.00(0.01)	1.00(0.98)	0.99(0.91)
hexanoate	0.31(0.00)	0.31(0.00)	0.69(1.00)	0.68(0.90)
Gly-L-Phe	0.06(0.00)	0.06(0.00)	0.94(1.00)	0.93(0.71)
N-acetyl-L-phenylalanine	0.00(0.00)	0.00(0.00)	1.00(1.00)	0.97(0.45)
4-methoxyphenylacetate	0.02(0.00)	0.02(0.00)	0.98(1.00)	0.97(0.95)
O-benzyl-L-serine	0.02(0.03)	0.00(0.00)	0.98(0.97)	0.07(0.02)
R-phenyllactic-acid	0.46(0.03)	0.46(0.00)	0.54(0.97)	0.53(0.01)
R-2-phenylbutyric-acid	0.00(0.00)	0.00(0.00)	1.00(1.00)	1.00(0.98)
N-acetyl-L-tyrosine	0.00(0.00)	0.00(0.00)	1.00(1.00)	0.93(0.35)
S-S-methoxy-S-trifluoromethylphenylacetic-acid	0.67(0.00)	0.67(0.00)	0.33(1.00)	0.33(0.99)
N-Cbz-L-alanine	0.00(0.12)	0.00(0.02)	1.00(0.88)	0.86(0.51)
3-phenylpropionate	0.10(0.00)	0.10(0.00)	0.90(1.00)	0.84(0.71)
N-Cbz-glycine	0.09(0.02)	0.09(0.01)	0.91(0.98)	0.48(0.07)
R-camphanic_acid	0.01(0.00)	0.00(0.00)	0.99(1.00)	0.96(0.78)
N-t-Boc-L-serine	0.00(0.02)	0.00(0.01)	1.00(0.98)	0.97(0.55)
3-4-hydroxyphenylpropionate	0.05(0.00)	0.05(0.00)	0.95(1.00)	0.92(0.68)
heptanoate	0.19(0.00)	0.19(0.00)	0.81(1.00)	0.77(0.58)
N-t-Boc-L-alanine	0.00(0.02)	0.00(0.00)	1.00(0.98)	0.99(0.86)
R-3-phenylbutyric-acid	0.68(0.00)	0.68(0.00)	0.31(1.00)	0.29(0.43)
4-phenylbutanoate	0.51(0.01)	0.50(0.00)	0.49(0.99)	0.43(0.54)
R-hexahydromandelic_acid	0.70(0.00)	0.70(0.00)	0.30(1.00)	0.29(0.74)
cyclohexylacetic_acid	0.17(0.00)	0.17(0.00)	0.83(1.00)	0.82(0.90)
flurbiprofen	0.00(0.02)	0.00(0.02)	1.00(0.98)	0.95(0.56)
1-naphthaleneacetate	0.00(0.00)	0.00(0.01)	1.00(0.99)	1.00(0.99)

Binding modes are defined as downstate (DS) and upstate binding mode (US). In the downstate mode, the guest prefers to have its polar functional group pointed toward the primary alcohols. In the upstate binding mode, the guest prefers to be pointed towards the secondary alcohols. The h-bond DS is the downstate mode where a hydrogen bond is formed between the primary alcohols and the polar functional group on the guest. The h-bond US is the upstate mode where a hydrogen bond is formed between the secondary alcohols and the polar functional group on the guest. Hydrogen bonds were defined using a distance cutoff of 4.0 Å between the carbon atom of the carboxylate group and the oxygen of the hydroxyl group.

TABLE S5: 2D chemical structures of the 5 experimental binders targeting the LEDGF binding site of HIV integrase.

AVX_17557_3	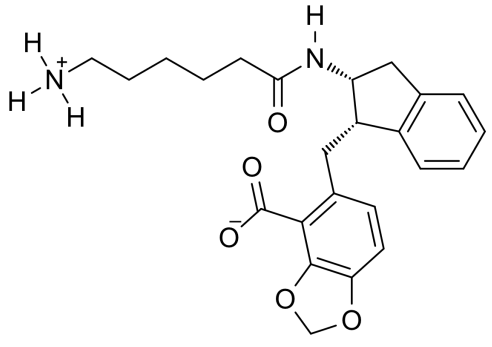
AVX17556_3	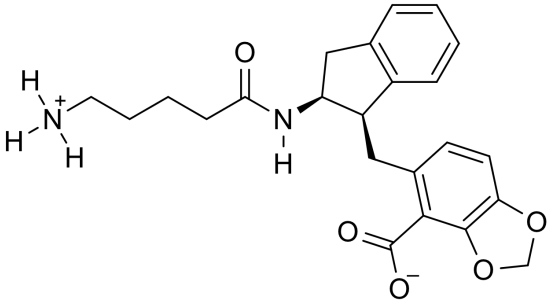
AVX17285_0	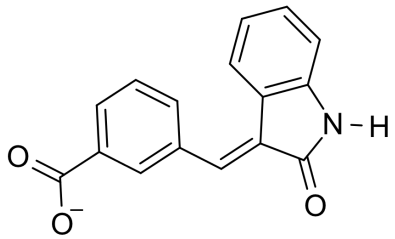

AVX38753_3_1	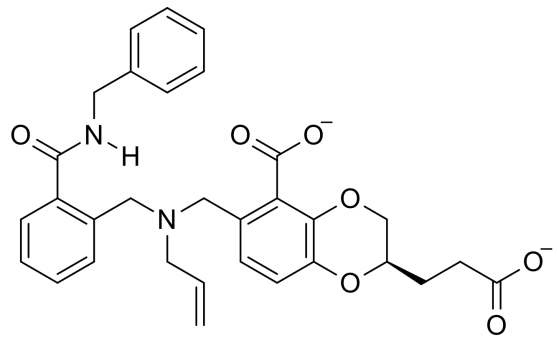
AVX101124_1	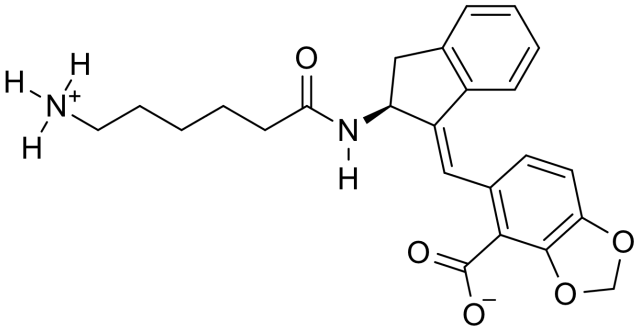

TABLE S6: 2D chemical structures of the 5 non-binders targeting the LEDGF binding site of HIV integrase.

AVX38784_7	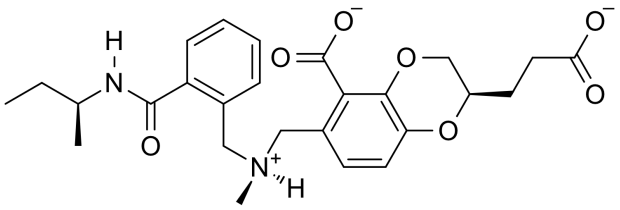
AVX38787_0	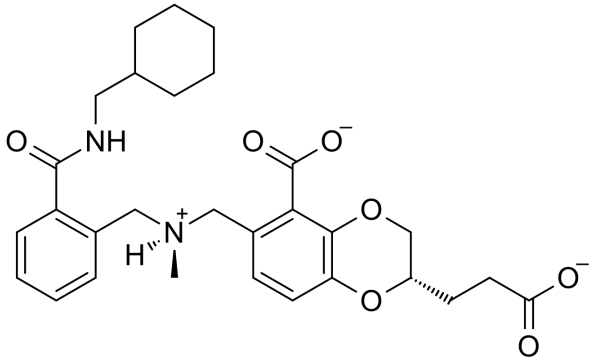
AVX38782_2	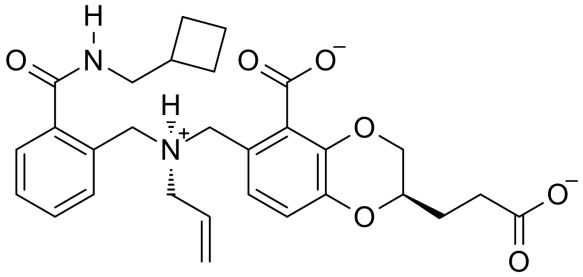
AVX38788_2	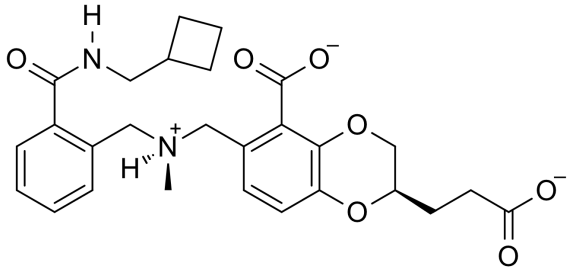

AVX38789_3	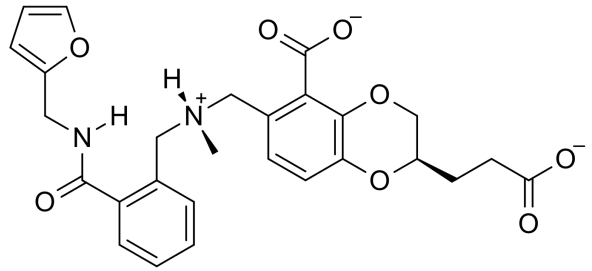

References

Bowers, K.J., E. Chow, Huageng Xu, R.O. Dror, M.P. Eastwood, B.A. Gregersen, J.L. Klepeis, et al. 2006. "Scalable Algorithms for Molecular Dynamics Simulations on Commodity Clusters." In *Proceedings of the ACM/IEEE SC 2006 Conference*, 43–43. doi:10.1109/SC.2006.54.

Chernick, Michael R. 2008. *Bootstrap Methods: A Guide for Practitioners and Researchers*. Hoboken, N.J.: Wiley-Interscience.

Gallicchio, Emilio, and Ronald M Levy. 2011. "Recent Theoretical and Computational Advances for Modeling Protein-Ligand Binding Affinities." *Advances in Protein Chemistry and Structural Biology* 85: 27–80. doi:10.1016/B978-0-12-386485-7.00002-8.

Gallicchio, Emilio, Kristina Paris, and Ronald M. Levy. 2009. "The AGBNP2 Implicit Solvation Model." *Journal of Chemical Theory and Computation* 5 (9): 2544–64. doi:10.1021/ct900234u.

Humphrey, W, A Dalke, and K Schulten. 1996. "VMD: Visual Molecular Dynamics." *Journal of Molecular Graphics* 14 (1): 33–38, 27–28.

Jorgensen, William L., Jayaraman Chandrasekhar, Jeffry D. Madura, Roger W. Impey, and Michael L. Klein. 1983. "Comparison of Simple Potential Functions for Simulating Liquid Water." *The Journal of Chemical Physics* 79 (2): 926–35. doi:10.1063/1.445869.

Nguyen, Crystal N, Tom Kurtzman Young, and Michael K Gilson. 2012. "Grid Inhomogeneous Solvation Theory: Hydration Structure and Thermodynamics of the Miniature Receptor cucurbit[7]uril." *The Journal of Chemical Physics* 137 (4): 044101. doi:10.1063/1.4733951.

Rekharsky, Mikhail, and Yoshihisa Inoue. 2000. "Chiral Recognition Thermodynamics of B-Cyclodextrin: The Thermodynamic Origin of Enantioselectivity and the Enthalpy−Entropy Compensation Effect." *Journal of the American Chemical Society* 122 (18): 4418–35. doi:10.1021/ja9921118.

Rekharsky, Mikhail V., and Yoshihisa Inoue. 1998. "Complexation Thermodynamics of Cyclodextrins." *Chemical Reviews* 98 (5): 1875–1918.

Rekharsky, Mikhail V, and Yoshihisa Inoue. 2002. "Solvent and Guest Isotope Effects on Complexation Thermodynamics of Alpha-, Beta-, and 6-Amino-6-Deoxy-Beta-Cyclodextrins." *Journal of the American Chemical Society* 124 (41): 12361–71.

Shirts, Michael R., and John D. Chodera. 2008. "Statistically Optimal Analysis of Samples from Multiple Equilibrium States." *The Journal of Chemical Physics* 129 (12): 124105. doi:10.1063/1.2978177.

Wickstrom, Lauren, Peng He, Emilio Gallicchio, and Ronald M. Levy. 2013. "Large Scale Affinity Calculations of Cyclodextrin Host–Guest Complexes: Understanding the Role of Reorganization in the Molecular Recognition Process." *Journal of Chemical Theory and Computation* 9 (7): 3136–50. doi:10.1021/ct400003r.